Spatial Modulation and Space-Time Shift Keying: Optimal Performance at a Reduced Detection Complexity

Chao Xu, *Student Member, IEEE,* Shinya Sugiura, *Senior Member, IEEE,* Soon Xin Ng, *Senior Member, IEEE,* and Lajos Hanzo *Fellow, IEEE*

***Abstract*—In this paper, we propose a comprehensive reduced-complexity detector both for hard-decision-aided as well as for the soft-decision-assisted Spatial Modulation (SM)/Space-Time Shift Keying (STSK). More explicitly, the detection of the SM scheme, which activates a single one out of M antennas to transmit a single LPSK/QAM symbol, may be carried out by detecting the antenna activation index m and the LPSK/QAM symbol s_l separately, so that the detection complexity may be reduced from the order of $O(M \cdot L)$ to the lower bound of $O(M + \log_2 L)$. However, the QAM aided STSK hard detection proposed in [1] results in a performance loss. Furthermore, the Max-Log-MAP algorithm proposed for soft STSK detection in [2] only takes into account the maximum *a posteriori* probabilities, which also imposed a performance degradation. Therefore, in this paper, we propose a novel solution for hard-decision-aided SM/STSK detection, which retains its optimal performance, despite its reduced detection complexity, when either LPSK or LQAM is employed. Furthermore, we propose the reduced-complexity Approx-Log-MAP algorithm conceived for the soft-decision-aided SM/STSK detector, in order to replace the sub-optimal Max-Log-MAP algorithm.**

***Index Terms*—Spatial Modulation, Space-Time Shift Keying, Reduced complexity design, Turbo detection.**

I. Introduction

MULTIPLE-Input Multiple-Output (MIMO) schemes are capable of providing wireless communication systems either with an increased capacity as in V-BLAST [3] and/or with an improved diversity gain [4]. However, full-search-based Maximum Likelihood (ML) MIMO detection may impose an excessive complexity in turbo detected schemes [5], [6]. As a remedy, Spatial Modulation (SM) was proposed in [7], where a single one out of M transmit antennas is activated to transmit a single LPSK/QAM symbol, so that a single-antenna-based detector may be invoked at the receiver. Furthermore, in order to benefit from a diversity gain, Space-Time Shift Keying (STSK) was proposed in [8], where one out of Q dispersion matrices was activated to disperse a single LPSK/QAM symbol to multiple antennas and time-slots. It was demonstrated in [8] that a low-complexity SM detector may be invoked for STSK detection.

Although the antenna activation index and the LPSK/QAM symbol are encoded independently in SM schemes, these two signals fade together. Hence, the attempt of detecting the two terms completely independently results in a significant performance loss [7], except when the Channel State Information (CSI) is known at the transmitter [9]. As a remedy, Space-Shift Keying (SSK) was proposed in [10], where simply the antenna activation index conveys the source information.

Recently, the reduced-complexity hard-decision PSK aided SM detection was proposed in the context of Differential STSK (DSTSK) [11], where the optimal performance was retained by taking into account the correlation between the antenna activation index and the LPSK symbol. Reduced-complexity hard-decision QAM aided STSK detection was proposed in [1], but a performance loss was imposed. Furthermore, the reduced-complexity Max-Log-MAP algorithm conceived for soft STSK detection was proposed in [2]. However, the Max-Log-MAP algorithm only considers the maximum *a posteriori* probabilities, which results in a sub-optimal performance. *Against this background, the novel contributions of this paper are as follows:*

(1) *Both PSK as well as QAM based reduced-complexity SM/STSK hard-decision-aided detection is proposed.*
(2) *For soft-decision-aided detection, a reduced-complexity Approx-Log-MAP algorithm is conceived for SM/STSK detection.*
(3) *Both the hard and the soft-decision-aided SM/STSK detectors proposed are generalized for different PSK/QAM constellations, which retain their optimal unimpaired detection capabilities, despite their reduced complexity.*

The remainder of this paper is organized as follows. The hard-decision aided SM detector is proposed in Section II, while the soft-decision-aided SM detector is conceived in Section III. The STSK scheme, which may invoke the SM detector is reviewed in Section IV. Our performance results are provided in Section V, while our conclusions are offered in Section VI.

Paper approved by C. Abou-Rjeily, the Editor for UWB and Diversity Methods of the IEEE Communications Society. Manuscript received April 12, 2012; revised June 26, 2012.

C. Xu, S. X. Ng and L. Hanzo are with the School of Electronics and Computer Science, University of Southampton, Southampton, SO17 1BJ, U.K. (e-mail: {cx1g08, sxn, lh}@ecs.soton.ac.uk).

S. Sugiura is currently with the Toyota Central R&D Labs, Inc., Aichi 480-1192, Japan (e-mail: sugiura@ieee.org).

The financial support of the RC-UK under the auspices of the India-UK Advanced Technology Centre (IU-ATC) and that of the EPSRC under the China-UK science bridge as well as that of the EU's Concerto project is gratefully acknowledged.

Digital Object Identifier 10.1109/TCOMM.2012.09.120251

The following notations are used throughout the paper. SM(M,N)-LPSK/QAM as well as V-BLAST(M,N)-LPSK/QAM denote the SM scheme and the V-BLAST scheme equipped with M transmit antennas and N receive antennas. Furthermore, a STSK scheme is denoted by the acronym of STSK(M,N,T,Q)-LPSK/QAM, where T and Q represent the number of symbol periods per transmission block and the total number of dispersion matrices employed, respectively.

II. Hard-Decision-Aided SM Detection

A. Conventional Hard-Decision-Aided SM Detection

For a SM scheme, the transmit vector is given by [7]:

$$\mathbf{S}_i = [\underbrace{0 \ \cdots \ 0}_{m-1}, s_l, \underbrace{0 \ \cdots \ 0}_{M-m}], \tag{1}$$

where $(\log_2 L)$ bits are assigned to modulate an LPSK/QAM symbol, while $(\log_2 M)$ bits are assigned to activate a single one out of a total of M transmit antennas.

The signal received by the N receive antennas may be modelled as:

$$\mathbf{Y}_n = \mathbf{S}_n \mathbf{H}_n + \mathbf{V}_n, \tag{2}$$

where $\mathbf{Y}_n \in \mathbb{C}^{1\times N}$ and $\mathbf{V}_n \in \mathbb{C}^{1\times N}$ refer to the received signal vector, and the Additive White Gaussian Noise (AWGN) vector, which has a zero mean and a variance of N_0, respectively, while $\mathbf{H}_n \in \mathbb{C}^{M\times N}$ models the Rayleigh fading channel.

Based on Eq. (2), the conventional MIMO detector, which operates on a matrix-by-matrix basis, may be expressed as:

$$\hat{\mathbf{S}}_n = \arg \min_{\mathbf{S}_i \in \mathbf{S}} \|\mathbf{Y}_n - \mathbf{S}_i \mathbf{H}_n\|^2, \tag{3}$$

where $\mathbf{S}$ stores all the SM codewords. Let us further extend the decision variable in Eq. (3) as:

$$\begin{aligned} \|\mathbf{Y}_n - \mathbf{S}_i \mathbf{H}_n\|^2 &= \mathrm{tr}\left\{(\mathbf{Y}_n - \mathbf{S}_i \mathbf{H}_n)(\mathbf{Y}_n - \mathbf{S}_i \mathbf{H}_n)^H\right\} \\ &= \|\mathbf{Y}_n\|^2 + \mu_m^2 |s_l|^2 - 2\mathrm{Re}\left\{s_l^* \mathbf{Y}_n \left(\mathbf{H}_n^m\right)^H\right\}, \end{aligned} \tag{4}$$

where the variable $\{\mu_m\}_{m=1}^M$ is given by $(\mu_m = \|\mathbf{H}_n^m\|)$, while $\{\mathbf{H}_n^m\}_{m=1}^M$ denotes the m-th row in $\mathbf{H}_n$. Eq. (4) leads to a decorrelating variable of:

$$\mathbf{Z}_n = \mathbf{Y}_n \left(\overline{\mathbf{H}}_n\right)^H, \tag{5}$$

where each row in the normalized fading matrix $\overline{\mathbf{H}}_n \in \mathbb{C}^{M\times N}$ is given by $\{\overline{\mathbf{H}}_n^m = \mathbf{H}_n^m/\mu_m\}_{m=1}^M$. It is well known that the decorrelating detector of V-BLAST imposes a performance loss. However, due to the fact that only a single transmit antenna was activated in our SM scheme, Eq. (4) now becomes equivalent to the vector-by-vector based detection metric of:

$$\|\mathbf{Z}_n - \mu_m \mathbf{S}_i\|^2 = \|\mathbf{Z}_n\|^2 + \mu_m^2 |s_l|^2 - 2\mathrm{Re}\{\mu_m \mathbf{Z}_n \left(\mathbf{S}_i\right)^H\}, \tag{6}$$

where we have $\mu_m \mathbf{Z}_n \left(\mathbf{S}_i\right)^H = s_l^* \mathbf{Y}_n \left(\mathbf{H}_n^m\right)^H$ according to Eq. (5), while both $\|\mathbf{Y}_n\|^2$ in Eq. (4) and $\|\mathbf{Z}_n\|^2$ in Eq. (6) are constants. Hence minimizing Eq. (4) and Eq. (6) are equivalent.

In conclusion, the vector-by-vector based SM detection may be formulated as:

$$\hat{\mathbf{S}}_n = \arg \min_{\mathbf{S}_i \in \mathbf{S}} \|\mathbf{Z}_n - \mu_m \mathbf{S}_i\|^2, \tag{7}$$

where μ_m may be found according to the antenna activation index m that corresponds to the tentative candidate $\mathbf{S}_i$.

B. Reduced-Complexity Hard-Decision-Aided SM Detection

Both the matrix-by-matrix based detection of Eq. (3) and the vector-by-vector based detection of Eq. (7) have a complexity order of $O(M \cdot L)$. In this section, we proceed further by detecting the antenna activation index m and the LPSK/QAM symbol index l separately, so that the detection complexity may be further reduced to the lower bound of $O(M + \log_2 L)$.

First of all, we further extend the vector-by-vector based detection metric of Eq. (7) as:

$$\begin{aligned} \|\mathbf{Z}_n - \mu_m \mathbf{S}_i\|^2 =& \|\mathbf{Z}_n\|^2 + \mu_m^2 |s_l|^2 - 2\mu_m \mathrm{Re}(Z_n^m)\mathrm{Re}(s_l) \\ & - 2\mu_m \mathrm{Im}(Z_n^m)\mathrm{Im}(s_l), \end{aligned} \tag{8}$$

where $\{Z_n^m\}_{m=1}^M$ denotes the m-th element in the decorrelating vector $\mathbf{Z}_n$. As a result, the LPSK/QAM aided SM detection of Eq. (7) may be simplifed to:

$$\begin{aligned} \{\hat{m}, \hat{l}\} = \arg \max_{m\in\bar{\mathbf{m}}, l\in\bar{l}} & \mathrm{Re}(\widetilde{Z}_n^m)\mathrm{Re}(s_l) + \mathrm{Im}(\widetilde{Z}_n^m)\mathrm{Im}(s_l) \\ & - \mu_m^2 |s_l|^2. \end{aligned} \tag{9}$$

where we have $\{\widetilde{Z}_n^m = 2\mu_m Z_n^m\}_{m=1}^M$, while $\bar{\mathbf{m}}$ and $\bar{l}$ store the antenna activation indices and LPSK/QAM symbol indices, respectively. The constant of $\|\mathbf{Z}_n\|^2$ seen in Eq. (8) is discarded.

In order to detect m and l separately, we have to drop the LPSK/QAM index l in Eq. (9), when detecting the antenna activation index m. Let us consider QPSK aided SM detection as an example, which has a PSK constellation set of $\{\pm\frac{1}{\sqrt{2}} \pm j\frac{1}{\sqrt{2}}\}$[1]. For a specific antenna index m, the maximum metric over all QPSK constellations is given by:

$$\begin{aligned} d_m &= \max_{l\in\bar{l}} \left\{\pm\frac{\mathrm{Re}(\widetilde{Z}_n^m)}{\sqrt{2}} \pm \frac{\mathrm{Im}(\widetilde{Z}_n^m)}{\sqrt{2}} - \mu_m^2\right\} \\ &= \left|\frac{\mathrm{Re}(\widetilde{Z}_n^m)}{\sqrt{2}}\right| + \left|\frac{\mathrm{Im}(\widetilde{Z}_n^m)}{\sqrt{2}}\right| - \mu_m^2, \end{aligned} \tag{10}$$

which is evaluated by a single equation instead of comparing all the $(L = 4)$ QPSK constellations. As a result, the optimum antenna activation index $\hat{m}$ may be found by searching for the maximum metric over all the M candidates $\{d_m\}_{m=1}^M$, regardless of which particular QPSK symbol was transmitted, which may be expressed as:

$$\hat{m} = \arg \max_{m\in\bar{\mathbf{m}}} d_m, \tag{11}$$

and then the corresponding $(\log_2 M)$ bits $\{\hat{b}_k\}_{k=\log_2 L+1}^{\log_2 I}$ assigned to activate $\hat{m}$ may be obtained accordingly, where $(I = M \cdot L)$ denotes the total number of SM codewords. Having determined the optimum $\hat{m}$, the $(\log_2 L)$ bits $\{\hat{b}_k\}_{k=1}^{\log_2 L}$

[1]We deliberately rotated all the constellations of LPSK ($L \geq 4$) in [12] anti-clockwise by a phase of $\frac{\pi}{L}$, so that there are exactly $L/4$ constellation points in each quadrant. This feature will be beneficial for reducing the complexity of the soft PSK aided SM/STSK detection.

assigned to modulate the QPSK symbol may be detected as:

$$\begin{aligned}\hat{b}_1 &= \begin{cases} 1, & \text{if } \mathrm{Im}(\widetilde{Z}_n^{\hat{m}}) < 0 \\ 0, & \text{otherwise} \end{cases}, \\ \hat{b}_2 &= \begin{cases} 1, & \text{if } \mathrm{Re}(\widetilde{Z}_n^{\hat{m}}) < 0 \\ 0, & \text{otherwise} \end{cases}. \end{aligned} \tag{12}$$

It can be seen that Eqs. (11) and (12) reduces the QPSK aided SM detection complexity from the order of $O(M \cdot 4)$ to $O(M + 2)$ by detecting the antenna index and the QPSK symbol separately.

Similarly, when Square 16QAM was employed, the maximum metrics $\{d_m\}_{m=1}^{M}$ seen in Eq. (11) may be obtained by testing the real and the imaginary parts of the LQAM constellation separately, which may be expressed as:

$$\begin{aligned} d_m^{Re1} &= \max \left\{ \pm \frac{1}{\sqrt{10}} \mathrm{Re}(\widetilde{Z}_n^m) - \frac{1}{10}\mu_m^2 \right\} \\ &= \left| \frac{1}{\sqrt{10}} \mathrm{Re}(\widetilde{Z}_n^m) \right| - \frac{1}{10}\mu_m^2, \\ d_m^{Re2} &= \max \left\{ \pm \frac{3}{\sqrt{10}} \mathrm{Re}(\widetilde{Z}_n^m) - \frac{9}{10}\mu_m^2 \right\} \\ &= \left| \frac{3}{\sqrt{10}} \mathrm{Re}(\widetilde{Z}_n^m) \right| - \frac{9}{10}\mu_m^2, \\ d_m^{Im1} &= \max \left\{ \pm \frac{1}{\sqrt{10}} \mathrm{Im}(\widetilde{Z}_n^m) - \frac{1}{10}\mu_m^2 \right\} \\ &= \left| \frac{1}{\sqrt{10}} \mathrm{Im}(\widetilde{Z}_n^m) \right| - \frac{1}{10}\mu_m^2, \\ d_m^{Im2} &= \max \left\{ \pm \frac{3}{\sqrt{10}} \mathrm{Im}(\widetilde{Z}_n^m) - \frac{9}{10}\mu_m^2 \right\} \\ &= \left| \frac{3}{\sqrt{10}} \mathrm{Im}(\widetilde{Z}_n^m) \right| - \frac{9}{10}\mu_m^2, \end{aligned} \tag{13}$$

where each one of them only has to be evaluated once. Furthermore, for a specific antenna index m, the maximum metric is given by:

$$d_m = \max_{i \in \{1,2\}} d_m^{Re_i} + \max_{j \in \{1,2\}} d_m^{Im_j}. \tag{14}$$

Then the antenna activation index detection of Eq. (11) may be invoked, and a streamlined Square 16QAM detection may be carried out as follows:

$$\begin{aligned}\hat{b}_1 &= \begin{cases} 1, & \text{if } \mathrm{Im}(\widetilde{Z}_n^{\hat{m}}) < 0 \\ 0, & \text{otherwise} \end{cases}, \\ \hat{b}_2 &= \begin{cases} 1, & \text{if } \hat{j} = 1 \text{ for } d_{\hat{m}} \\ 0, & \text{otherwise} \end{cases}, \\ \hat{b}_3 &= \begin{cases} 1, & \text{if } \mathrm{Re}(\widetilde{Z}_n^{\hat{m}}) < 0 \\ 0, & \text{otherwise} \end{cases}, \\ \hat{b}_4 &= \begin{cases} 1, & \text{if } \hat{i} = 1 \text{ for } d_{\hat{m}} \\ 0, & \text{otherwise} \end{cases}, \end{aligned} \tag{15}$$

where the optimum 16QAM magnitude indices $\hat{i}$ and $\hat{j}$ have been obtained in Eq. (14).

We summarize the hard-decision Square LQAM aided SM detection in Table I. Furthermore, when either a high-order LPSK ($L > 4$) or a Star L-QAM constellation [13], [14] is employed, the real and imaginary parts of the decorrelating variable $\widetilde{Z}_n^m$ cannot be detected separately. However, as long as we have two bits, which determine the signs of the real and imaginary parts of the transmitted symbol, a similar detection algorithm may be conceived, which is summarized in Table II[2].

We note that the low-complexity SM detection proposed in [7] always achieves the complexity lower bound of $O(M + \log_2 L)$, because it detects the antenna index as $\hat{m} = \arg \max_{m \in \mathbf{m}} |Z_n^m|^2$, which may result in an erroneous decision and hence the LPSK/QAM demodulator may be misled into detecting the wrong symbol. By contrast, our proposed SM detection characterized in this section retains the same detection capability as the full-search-based MIMO detection of Eq. (3), because the proposed antenna index detection takes into account which particular LPSK/QAM scheme was employed. As a result, only the family of 1PSK[3]/BPSK/QPSK aided SM detection arrangements may achieve the complexity lower bounds of $O(M)$, $O(M+1)$ and $O(M+2)$, respectively, where the special case of hard-decision 1PSK/BPSK aided SM detection is summarized in the Appendix. The high-order Square LQAM aided SM detection presented in Table I has a complexity order of $O(\sqrt{L} \cdot M + 4)$, where a total number of $\sqrt{L}$ comparisons have been made for estimating $\{d_m\}_{m=1}^{M}$, while the streamlined Square LQAM demodulator detects the $\log_2 L$ bits by simply testing the two variables of $\mathrm{Re}(\widetilde{Z}_n^{\hat{m}})$ and $\mathrm{Im}(\widetilde{Z}_n^{\hat{m}})$, as well as the two magnitude indices $\hat{i}$ and $\hat{j}$. Similarly, the generalized LPSK/QAM aided SM detection complexity order of Table II is given by $O(\frac{L}{4} \cdot M + 3)$, which is higher than that of Table I.

When the number of bits per Square LQAM symbol is an odd number, the Algorithm 1 shown in Table I may be readily modified, where the real *positive* PAM magnitudes have $\sqrt{2L}/2$ candidates, while the imaginary *positive* PAM magnitudes have $\sqrt{L/2}/2$ candidates. Furthermore, it was shown in [15] that Cross L-QAM constellations actually have a better performance compared to Square L-QAM schemes. We note that the Algorithm 2 of Table II may be adopted for detecting the family of Cross LQAM aided SM schemes.

III. Soft-Decision-Aided SM Detection

A. Conventional Soft-Decision-Aided SM Detection

For the soft-decision-aided detection, the classic Log-MAP algorithm is given by [16]:

$$L_p(b_k) = \ln \left[\frac{\sum_{\mathbf{S}_i \in \mathbf{S}_{b_k=1}} \exp(d_i)}{\sum_{\mathbf{S}_i \in \mathbf{S}_{b_k=0}} \exp(d_i)} \right], \tag{16}$$

where $L_p(b_k)$ refers to the *a posteriori* LLRs, while $\mathbf{S}_{b_k=1}$ and $\mathbf{S}_{b_k=0}$ denote the SM codeword sets, when the specific bit b_k is fixed to 1 and 0, respectively. The probability metric $\{d_i\}_{i=1}^{I}$ in Eq. (16) is given by:

$$d_i = -\frac{\|\mathbf{Y}_n - \mathbf{S}_i \mathbf{H}_n\|^2}{N_0} + \sum_{j=1}^{\log_2 I} b_j L_a(b_j), \tag{17}$$

[2]We deliberately rotate all the Star L-QAM constellations of [13], [14] anti-clockwise by a phase angle of (π/L_P), where L_A and L_P refers to the number of constellation rings and the number of phasors, respectively.

[3]We note that the 1PSK aided SM detection refers to the SSK scheme of [10], where no source information was assigned to the L-PSK modulation.

TABLE I
ALGORITHM 1: REDUCED-COMPLEXITY HARD-DECISION SQUARE LQAM AIDED SM DETECTION.

(1) Define the metrics that tests the real and imaginary parts separately as:
$$d_m^{\mathrm{Re}_i} = \left|A_i \mathrm{Re}(\widetilde{Z}_n^m)\right| - A_i^2\mu_m^2, \quad d_m^{\mathrm{Im}_i} = \left|A_i \mathrm{Im}(\widetilde{Z}_n^m)\right| - A_i^2\mu_m^2,$$
where $\{A_i\}_{i=1}^{\sqrt{L}/2}$ are the positive real PAM magnitudes on the x-axis and y-axis of Square LQAM constellation diagram.

(2) For a specific m, the maximum metric over all Square LQAM constellations is given by testing the real and imaginary parts separately as:
$$d_m = \max_{i\in\{1,\cdots,\sqrt{L}/2\}} d_m^{\mathrm{Re}_i} + \max_{j\in\{1,\cdots,\sqrt{L}/2\}} d_m^{\mathrm{Im}_j},$$
where the optimum PAM magnitudes indices $\hat{i}$ and $\hat{j}$ obtained for each $\{d_m\}_{m=1}^M$ may be recorded.

(3) The optimum antenna activation index may be found by:
$$\hat{m} = \arg \max_{m\in\bar{\mathbf{m}}} d_m,$$
and then the corresponding $(\log_2 M)$ bits $\{\hat{b}_k\}_{k=\log_2 L+1}^{\log_2 I}$ assigned to activate $\hat{m}$ may be obtained accordingly.

(4) The first bit and the $(\frac{\log_2 L}{2}+1)$-th bit which determine the signs may be demodulated as:
$$\hat{b}_1 = \begin{cases} 1, & \text{if } \mathrm{Im}(\widetilde{Z}_n^{\hat{m}}) < 0 \\ 0, & \text{otherwise} \end{cases}, \quad \hat{b}_{(\log_2 L)/2+1} = \begin{cases} 1, & \text{if } \mathrm{Re}(\widetilde{Z}_n^{\hat{m}}) < 0 \\ 0, & \text{otherwise} \end{cases}.$$

(5) For the $(\log_2 L - 2)$ bits $\{\hat{b}_k\}_{k=2}^{(\log_2 L)/2}$ and $\{\hat{b}_k\}_{(\log_2 L)/2+2}^{\log_2 L}$ which determine the magnitudes, the optimum bit mapping is corresponding to the imaginary and real magnitude indices $\hat{j}$ and $\hat{i}$, respectively, which were obtained when estimating $d_{\hat{m}}$ in Step (2).

TABLE II
ALGORITHM 2: REDUCED-COMPLEXITY HARD-DECISION GENERAL LPSK/QAM AIDED SM DETECTION.

(1) Define the new testing metrics as:
$$d_m^i = \left|A_i \mathrm{Re}(\widetilde{Z}_n^m)\right| + \left|B_i \mathrm{Im}(\widetilde{Z}_n^m)\right| - (A_i^2 + B_i^2)\mu_m^2,$$
where $\{(A_i, B_i)\}_{i=1}^{L/4}$ denote the coordinates of the LPSK/QAM constellation points in the first quadrant, and $(A_i^2 + B_i^2 = 1)$ is a constant when LPSK is employed.

(2) For a specific m, the maximum metric over all LPSK/QAM constellations is given by:
$$d_m = \max_{i\in\{1,\cdots,L/4\}} d_m^i,$$
where the optimum constellation index $\hat{i}$ obtained for each $\{d_m\}_{m=1}^M$ may be recorded.

(3) The optimum antenna activation index may be found by:
$$\hat{m} = \arg \max_{m\in\bar{\mathbf{m}}} d_m,$$
and then the corresponding $(\log_2 M)$ bits $\{\hat{b}_k\}_{k=\log_2 L+1}^{\log_2 I}$ assigned to activate $\hat{m}$ may be obtained accordingly.

(4) The first bit and the second bit which determine the signs may be demodulated as:
$$\hat{b}_1 = \begin{cases} 1, & \text{if } \mathrm{Im}(\widetilde{Z}_n^{\hat{m}}) < 0 \\ 0, & \text{otherwise} \end{cases}, \quad \hat{b}_2 = \begin{cases} 1, & \text{if } \mathrm{Re}(\widetilde{Z}_n^{\hat{m}}) < 0 \\ 0, & \text{otherwise} \end{cases}.$$

(5) For the rest $(\log_2 L - 2)$ bits $\{\hat{b}_k\}_{k=3}^{\log_2 L}$ which determine the magnitudes, the optimum bit mapping arrangement is corresponding to the optimum constellation index $\hat{i}$, which were obtained when estimating $d_{\hat{m}}$ in Step (2).

where $\{L_a(b_j)\}_{j=1}^{\log_2 I}$ refers to the *a priori* LLRs gleaned from a channel decoder. Similar to Eq. (7), Eq. (17) may be calculated on a vector-by-vector basis as:

$$d_i = -\frac{\|\mathbf{Z}_n - \mu_m \mathbf{S}_i\|^2}{N_0} + \sum_{j=1}^{\log_2 I} b_j L_a(b_j). \tag{18}$$

According to our previous results in Eqs. (4) and (6), the differences between Eq. (17) and Eq. (18) are all constants, which are eliminated by the division operation in Eq. (16).

The Log-MAP algorithm may be simplified by the Max-Log-MAP algorithm as [16]:

$$L_p(b_k) = \max_{\mathbf{S}_i\in\mathbf{S}_{b_k=1}} (d_i) - \max_{\mathbf{S}_i\in\mathbf{S}_{b_k=0}} (d_i). \tag{19}$$

Since only the pair of maximum *a posteriori* probabilities are taken into account in Eq. (19), the Max-Log-MAP algorithm imposes a slight performance degradation. In order to compensate for this performance loss, the Approx-Log-MAP algorithm was introduced as [17]:

$$L_p(b_k) = \mathrm{jac}_{\mathbf{S}_i\in\mathbf{S}_{b_k=1}} (d_i) - \mathrm{jac}_{\mathbf{S}_i\in\mathbf{S}_{b_k=0}} (d_i), \tag{20}$$

where *jac* denotes the Jacobian algorithm, which may be expressed as [6]:

$$\mathrm{jac}(d_1, d_2) = \max\ \{d_1, d_2\} + \Gamma\{|d_1 - d_2|\}, \tag{21}$$

where the additional term of $\Gamma\{|d_1 - d_2|\}$ takes into account the difference between d_1 and d_2 according to a lookup table [6]. When comparing two variables, which have the same magnitudes but are associated with the opposite signs, the maximization operation gives the simple result of $(\max\{t, -t\} = |t|)$. Similarly, we define the special case for the Jacobian algorithm as:

$$\Lambda(|t|) = \mathrm{jac}(t, -t) = |t| + \Gamma\{2|t|\}. \tag{22}$$

In the following section, we aim for invoking Eq. (22) for a streamlined algorithm.

B. Reduced-Complexity Soft-Decision-Aided SM Detection

For producing a single soft-bit output, the conventional SM detectors have to estimate a total number of $(I = M \cdot L)$ *a posteriori* probability metrics $\{d_i\}_{i=1}^I$. In this section, we once again aim for detecting m and l separately. For the $(\log_2 M)$ bits which are assigned to the antenna index, the detection complexity order of the Approx-Log-MAP algorithm of Eq. (20) may be lower bounded by $O(M)$, where ideally the antenna activation index detector does not have to visit the L-element PSK/QAM constellations set. Meanwhile, for the $(\log_2 L)$ bits which are assigned to an LPSK/QAM symbol, the detection complexity may be lower bounded by $O(2M)$, where ideally the antenna activation index detector only has to be invoked twice according to the updated LPSK/QAM subsets, when a specific bit b_k is set to 1 and 0, respectively.

Similar to Eq. (8), the *a posteriori* probability evaluation of Eq. (18) may be extended as:

$$d_{m,l} = \frac{\mathrm{Re}(\widetilde{Z}_n^m)\mathrm{Re}(s_l)}{N_0} + \frac{\mathrm{Im}(\widetilde{Z}_n^m)\mathrm{Im}(s_l)}{N_0} - \frac{\mu_m^2|s_l|^2}{N_0} + \sum_{j=1}^{\log_2 I} b_j L_a(b_j), \tag{23}$$

where a constant of $\left(-\frac{\|\mathbf{Z}_n\|^2}{N_0}\right)$ is discarded from Eq. (18).

For the $(\log_2 M)$ bits which are assigned to the antenna index, the soft decisions produced by Eq. (20) may be expressed as:

$$L_p(b_k) = \mathrm{jac}_{m\in\bar{\mathbf{m}}_{b_k=1}}(d_m) - \mathrm{jac}_{m\in\bar{\mathbf{m}}_{b_k=0}}(d_m), \tag{24}$$

where $\bar{\mathbf{m}}_{b_k=1}$ and $\bar{\mathbf{m}}_{b_k=0}$ refer to the index set for m, when the specific bit $\{b_k\}_{k=\log_2 L+1}^{\log_2 I}$ is fixed to 1 and 0, respectively. For a specific antenna index m seen in Eq. (24), we have to obtain the probability of $d_m = \mathrm{jac}_{l\in\bar{l}}(d_{m,l})$. Considering QPSK as an example, the *a posteriori* probability for each antenna index is given by Eq. (25), where the *a priori* probability of the antenna index m is given by $\left[\mathrm{Pr}_m = \sum_{j=\log_2 L+1}^{\log_2 I} b_j L_a(b_j)\right]$. Let us define two variables to test the real and the imaginary part separately as:

$$t_m^{Re} = \frac{\mathrm{Re}(\widetilde{Z}_n^m)}{\sqrt{2}N_0} - \frac{L_a(b_2)}{2}, \quad t_m^{Im} = \frac{\mathrm{Im}(\widetilde{Z}_n^m)}{\sqrt{2}N_0} - \frac{L_a(b_1)}{2}, \tag{26}$$

so that Eq. (25) may be further expressed as:

$$d_m = \Lambda(|t_m^{Re}|) + \Lambda(|t_m^{Im}|) - \frac{\mu_m^2}{N_0} + \mathrm{Pr}_m, \tag{27}$$

where a constant of $\frac{L_a(b_1)+L_a(b_2)}{2}$ is discarded from Eq. (25). Therefore, the Approx-Log-MAP algorithm of Eq. (24) may be invoked by using the *a posteriori* probabilities $\{d_m\}_{m=1}^M$ of Eq. (27) in order to detect the last $(\log_2 M)$ bits $\{L_p(b_k)\}_{k=\log_2 L+1}^{\log_2 I}$.

When the Max-Log-MAP algorithm is invoked, the *a posteriori* probability of Eq. (27) may be further simplified as:

$$d_m = |t_m^{Re}| + |t_m^{Im}| - \frac{\mu_m^2}{N_0} + \mathrm{Pr}_m, \tag{28}$$

while the $(\log_2 M)$ soft bit decisions may be made without invoking the Jacobian algorithms as:

$$L_p(b_k) = \max_{m\in\bar{\mathbf{m}}_{b_k=1}}(d_m) - \max_{m\in\bar{\mathbf{m}}_{b_k=0}}(d_m). \tag{29}$$

It can be seen that the detection algorithms of Eqs. (24) and (29) only have to estimate and compare the M *a posteriori* probabilities $\{d_m\}_{m=1}^M$ of Eqs. (27) and (28), respectively. Therefore the complexity order has been reduced from $O(M \cdot L)$ to $O(M)$.

For the first $(\log_2 L)$ bits, when a specific bit is set to 1 or 0 as seen in Eq. (20), the LPSK constellation set has to be updated. For the sake of producing the first soft bit decision, the Approx-Log-MAP algorithm of Eq. (20) is formulated as:

$$\begin{aligned} L_p(b_1) &= \mathrm{jac}_{m\in\bar{\mathbf{m}}}\left[\mathrm{jac}_{l\in\bar{l}_{b_1=1}}(d_{m,l})\right] \\ &\quad - \mathrm{jac}_{m\in\bar{\mathbf{m}}}\left[\mathrm{jac}_{l\in\bar{l}_{b_1=0}}(d_{m,l})\right] \\ &= \mathrm{jac}_{m\in\bar{\mathbf{m}}}\left[\Lambda(|t_m^{Re}|) - t_m^{Im} - \frac{\mu_m^2}{N_0} + \mathrm{Pr}_m\right] \\ &\quad - \mathrm{jac}_{m\in\bar{\mathbf{m}}}\left[\Lambda(|t_m^{Re}|) + t_m^{Im} - \frac{\mu_m^2}{N_0} + \mathrm{Pr}_m\right], \end{aligned} \tag{30}$$

where the imaginary term of $\Lambda(|t_m^{Im}|)$ in Eq. (27) is replaced by $(-t_m^{Im})$ and (t_m^{Im}), when b_1 is fixed to 1 and 0, respectively. Similarly, the second soft bit decision is given by:

$$\begin{aligned} L_p(b_2) &= \mathrm{jac}_{m\in\bar{\mathbf{m}}}\left[-t_m^{Re} + \Lambda(|t_m^{Im}|) - \frac{\mu_m^2}{N_0} + \mathrm{Pr}_m\right] \\ &\quad - \mathrm{jac}_{m\in\bar{\mathbf{m}}}\left[t_m^{Re} + \Lambda(|t_m^{Im}|) - \frac{\mu_m^2}{N_0} + \mathrm{Pr}_m\right]. \end{aligned} \tag{31}$$

The corresponding Max-Log-MAP algorithm may be obtained by replacing all the Jacobian operations of jac by the maximization operation of $\max$, while the special case of $\Lambda(|t|)$ may be replaced by $|t|$.

The complexity order of Eqs. (30) and (31) is $O(2M)$, where the antenna index detector is invoked twice according to the updated symbol set, when the specific bit is fixed to 1 and 0.

Let us further consider the example of Square 16QAM aided SM detection, where the *a posteriori* probability of a specific antenna index is given by:

$$d_m = \mathrm{jac}_{l\in\bar{l}}(d_{m,l}) = d_m^{Re} + d_m^{Im} + \mathrm{Pr}_m, \tag{32}$$

where we aim for testing the real and the imaginary part separately. The real part d_m^{Re} in Eq. (32) may be further extended as:

$$\begin{aligned} d_m^{Re} &= \mathrm{jac}\left\{\begin{array}{l} \frac{\mathrm{Re}(\widetilde{Z}_n^m)}{\sqrt{10}N_0} + L_a(b_4) - \frac{\mu_m^2}{10N_0}, \\ -\frac{\mathrm{Re}(\widetilde{Z}_n^m)}{\sqrt{10}N_0} + L_a(b_3) + L_a(b_4) - \frac{\mu_m^2}{10N_0}, \\ \frac{3\mathrm{Re}(\widetilde{Z}_n^m)}{\sqrt{10}N_0} - \frac{9\mu_m^2}{10N_0}, \\ \frac{-3\mathrm{Re}(\widetilde{Z}_n^m)}{\sqrt{10}N_0} + L_a(b_3) - \frac{9\mu_m^2}{10N_0} \end{array}\right\} \\ &= \mathrm{jac}\left\{\begin{array}{l} \Lambda(|t_m^{Re1}|) + L_a(b_4) - \frac{\mu_m^2}{10N_0}, \\ \Lambda(|t_m^{Re2}|) - \frac{9\mu_m^2}{10N_0} \end{array}\right\} + \frac{L_a(b_3)}{2} \\ &= \mathrm{jac}\left\{d_m^{Re1},\ d_m^{Re2}\right\} + \frac{L_a(b_3)}{2}, \end{aligned} \tag{33}$$

where the constant of $\frac{L_a(b_3)}{2}$ may be deleted, while the two test-variables are defined as:

$$t_m^{Re1} = \frac{\mathrm{Re}(\widetilde{Z}_n^m)}{\sqrt{10}N_0} - \frac{L_a(b_3)}{2}, \quad t_m^{Re2} = \frac{3\mathrm{Re}(\widetilde{Z}_n^m)}{\sqrt{10}N_0} - \frac{L_a(b_3)}{2}. \tag{34}$$

Similarly, the imaginary term d_m^{Im} in Eq. (32) may be formulated as:

$$\begin{aligned} d_m^{Im} &= \mathrm{jac}\left\{\begin{array}{l} \Lambda(|t_m^{Im1}|) + L_a(b_2) - \frac{\mu_m^2}{10N_0}, \\ \Lambda(|t_m^{Im2}|) - \frac{9\mu_m^2}{10N_0} \end{array}\right\} \\ &= \mathrm{jac}\left\{d_m^{Im1},\ d_m^{Im2}\right\}, \end{aligned} \tag{35}$$

$$d_m = \text{jac}_{l\in\bar{l}} \left\{ \begin{array}{l} \frac{\text{Re}(\widetilde{Z}_n^m)}{\sqrt{2}N_0} + \frac{\text{Im}(\widetilde{Z}_n^m)}{\sqrt{2}N_0} - \frac{\mu_m^2}{N_0} + \text{Pr}_m \\ -\frac{\text{Re}(\widetilde{Z}_n^m)}{\sqrt{2}N_0} + \frac{\text{Im}(\widetilde{Z}_n^m)}{\sqrt{2}N_0} + L_a(b_2) - \frac{\mu_m^2}{N_0} + \text{Pr}_m \\ \frac{\text{Re}(\widetilde{Z}_n^m)}{\sqrt{2}N_0} - \frac{\text{Im}(\widetilde{Z}_n^m)}{\sqrt{2}N_0} + L_a(b_1) - \frac{\mu_m^2}{N_0} + \text{Pr}_m \\ -\frac{\text{Re}(\widetilde{Z}_n^m)}{\sqrt{2}N_0} - \frac{\text{Im}(\widetilde{Z}_n^m)}{\sqrt{2}N_0} + L_a(b_1) + L_a(b_2) - \frac{\mu_m^2}{N_0} + \text{Pr}_m \end{array} \right\}. \quad (25)$$

where the constant of $\frac{L_a(b_1)}{2}$ is discarded, while the two test-variables are defined as:

$$t_m^{Im1} = \frac{\text{Im}(\widetilde{Z}_n^m)}{\sqrt{10}N_0} - \frac{L_a(b_1)}{2}, \quad t_m^{Im2} = \frac{3\text{Im}(\widetilde{Z}_n^m)}{\sqrt{10}N_0} - \frac{L_a(b_1)}{2}. \quad (36)$$

Therefore, for the Approx-Log-MAP algorithm, the antenna index detector of Eq. (24) may be invoked by utilizing the M *a posteriori* probabilities $\{d_m\}_{m=1}^{M}$ defined in Eq. (32), in order to produce the $(\log_2 M)$ soft bit decisions $\{L_p(b_k)\}_{k=\log_2 L+1}^{\log_2 I}$. The complexity order is reduced from $O(M \cdot 16)$ to $O(M \cdot 4)$, where four comparison operations have been made in Eqs. (33) and (35).

When the first bit b_1 which determines the sign of the imaginary part of a Square 16QAM symbol is fixed to 1 or 0, $\{\Lambda(|t_m^{Imi}|)\}_{i=1}^{2}$ seen in Eq. (35) may be replaced by $\{-t_m^{Imi}\}_{i=1}^{2}$ and $\{t_m^{Imi}\}_{i=1}^{2}$, respectively. More explicitly, the Approx-Log-MAP produces the first soft bit as Eq. (37), where d_m^{Re} does not have to be estimated again. The complexity order of detecting $L_a(b_1)$ is given by $O(M \cdot 4)$.

When the second bit b_2 which determines the magnitude of the imaginary part of a Square 16QAM symbol is fixed to 1 or 0, Eq. (35) should be updated as $d_m^{Im} = d_m^{Im1}$ or $d_m^{Im} = d_m^{Im2}$, respectively. As a result, the second soft bit decision is given by:

$$\begin{aligned} L_p(b_2) = &\text{jac}_{m\in\bar{\mathbf{m}}} \ (d_m^{Re} + d_m^{Im1} + Pr_m) \\ &- \text{jac}_{m\in\bar{\mathbf{m}}} \ (d_m^{Re} + d_m^{Im2} + Pr_m), \end{aligned} \quad (38)$$

where there is no new variable to evaluate, i.e. only additions and comparisons are made in Eq. (38). Therefore, the complexity order of detecting the second bit is given by $O(M \cdot 2)$.

Similarly, the third bit which determines the sign of the real part of a Square 16QAM symbol may be detected by the Approx-Log-MAP algorithm as:

$$L_p(b_3) = \text{jac}_{m\in\bar{\mathbf{m}}} \ \left(d_m^{b_3=1}\right) - \text{jac}_{m\in\bar{\mathbf{m}}} \ \left(d_m^{b_3=0}\right), \quad (39)$$

where $d_m^{b_3=1}$ and $d_m^{b_3=0}$ are obtained by replacing $\{\Lambda(|t_m^{Rei}|)\}_{i=1}^{2}$ seen in d_m^{Re} of Eq. (33) by $\{-t_m^{Rei}\}_{i=1}^{2}$ and $\{t_m^{Rei}\}_{i=1}^{2}$, respectively.

Furthermore, the fourth bit, which modulates the magnitude of the real part of a Square 16QAM symbol may be detected as:

$$\begin{aligned} L_p(b_4) = &\text{jac}_{m\in\bar{\mathbf{m}}} \ (d_m^{Re1} + d_m^{Im} + Pr_m) \\ &- \text{jac}_{m\in\bar{\mathbf{m}}} \ (d_m^{Re2} + d_m^{Im} + Pr_m). \end{aligned} \quad (40)$$

We have summarized the Approx-Log-MAP conceived for Square LQAM aided SM detection in Table III, while the general LPSK/QAM aided SM detection is summarized in Table IV. The special case of 1PSK/BPSK aided SM detection is detailed in the Appendix. As discussed right after Eq. (31), the reduced-complexity Max-Log-MAP may be obtained accordingly.

For the $(\log_2 M)$ bits assigned to the antenna index, the 1PSK/BPSK/QPSK aided SM detection achieves the complexity order lower bound of $O(M)$, while the Square LQAM aided SM detection of Table III and the LPSK/QAM aided SM detection of Table IV have the complexity order of $O(\sqrt{L} \cdot M)$ and $O(\frac{L}{4} \cdot M)$, respectively. For the two specific bits, which determine the sign of the transmitted LPSK/QAM symbol, the BPSK/QPSK aided SM detection complexity is lower bounded by the order of $O(2M)$, while the Square LQAM aided SM detection complexity order and the general LPSK/QAM aided SM detection complexity order are given by $O(\sqrt{L} \cdot M)$ and $O(\frac{L}{2} \cdot M)$, respectively. For the remaining $(\log_2 L - 2)$ bits, which determine the specific magnitudes of the LPSK/QAM symbols, the complexity order of the Square LQAM aided SM detection and that of the general LPSK/QAM aided SM detection are given by $O(\frac{\sqrt{L}}{2} \cdot M)$ and $O(\frac{L}{4} \cdot M)$, respectively. In summary, the Square LQAM aided SM detection of Algorithm 3 has a lower complexity compared to Algorithm 4, where the latter applies to high-order LPSK, Star LQAM and Cross LQAM aided SM schemes.

IV. Space-Time Shift Keying

It was demonstrated in [8] that the SM detector may be invoked for STSK detection. In fact, a SM scheme may be seen as a special case of STSK in conjunction with $(T = 1)$ and $(Q = M)$ [18]. In this section, we summarize the STSK schemes having different parameters in three cases, so that our proposed reduced-complexity SM detector may be invoked accordingly.

A. STSK Encoding

For a STSK scheme, the $(T \times M)$-element transmission matrix is obtained by the so-called dispersion process [8] of $\left(\mathbf{S}_n = \widetilde{\mathbf{A}}_q s_l\right)$, where $\log_2 L$ bits are assigned to modulate a single LPSK/QAM symbol $\{s_l\}_{l=1}^{L}$, while $\log_2 Q$ bits are assigned to activate one out of a total number of Q dispersion matrices $\{\widetilde{\mathbf{A}}_q\}_{q=1}^{Q}$.

In order to obtain the optimum dispersion matrix set, $(\overline{T} \times \overline{T})$ full-rank unitary matrices are randomly generated, where we have $\left(\overline{T} = \max\{M, T\}\right)$. The set of dispersion matrices is obtained by taking the first T rows or the first M columns of the unitary matrices, for the case of $(M > T)$ and $(M < T)$, respectively. A constant of $(\sqrt{\frac{T}{M}})$ should be used for multiplying all the dispersion matrices, when we have $(M < T)$, so that the power constraint of $\left[\text{tr}(\widetilde{\mathbf{A}}_q \cdot \widetilde{\mathbf{A}}_q^H) = T\right]$ may be satisfied. The optimum dispersion matrices may be obtained by maximizing the minimum distance between STSK codewords as $\left(\max \ \{\det[(\mathbf{S}_f - \mathbf{S}_g)]\}_{min}\right)$ [8].

$$\begin{aligned} L_p(b_1) &= \text{jac}_{m\in\bar{\mathbf{m}}}\ \left(d_m^{b_1=1}\right) - \text{jac}_{m\in\bar{\mathbf{m}}}\ \left(d_m^{b_1=0}\right) \\ &= \text{jac}_{m\in\bar{\mathbf{m}}}\ \left\{d_m^{Re} + \text{jac}\left[\ -t_m^{Im1} + L_a(b_2) - \tfrac{1}{10}\mu_m^2,\quad -t_m^{Im2} - \tfrac{9}{10}\mu_m^2\ \right] + Pr_m\right\} \\ &\quad - \text{jac}_{m\in\bar{\mathbf{m}}}\ \left\{d_m^{Re} + \text{jac}\left[\ t_m^{Im1} + L_a(b_2) - \tfrac{1}{10}\mu_m^2,\quad t_m^{Im2} - \tfrac{9}{10}\mu_m^2\ \right] + Pr_m\right\}. \end{aligned} \tag{37}$$

TABLE III

ALGORITHM 3: REDUCED-COMPLEXITY APPROX-LOG-MAP ALGORITHM CONCEIVED FOR SQUARE LQAM AIDED SM DETECTION.

(1) Define the variables testing the real and imaginary parts of the decorrelating variable $\widetilde{Z}_n^m$ separately as:

$$t_m^{\text{Re}_i} = \frac{A_i \text{Re}(\tilde{Z}_n^m)}{N_0} - \frac{L_a\left(b_{(\log_2 L)/2+1}\right)}{2},\quad t_m^{\text{Im}_i} = \frac{A_i \text{Im}(\tilde{Z}_n^m)}{N_0} - \frac{L_a(b_1)}{2},$$

where $\{A_i\}_{i=1}^{\sqrt{L}/2}$ are the positive real PAM magnitudes on the x-axis and y-axis of Square LQAM constellation diagram.

(2) The *a posteriori* probability of a specific antenna index m is given by:

$$d_m = d_m^{Re} + d_m^{Im} + \text{Pr}_m,$$

where the *a priori* probability of the antenna index m is given by $\text{Pr}_m = \sum_{j=\log_2 L+1}^{\log_2 I} b_j L_a(b_j)$, while the real and imaginary terms of the decision metric are given by:

$$d_m^{Re} = \text{jac}_{i\in\{1,\cdots,\sqrt{L}/2\}}\ \left(d_m^{Re_i}\right),\quad d_m^{Im} = \text{jac}_{i\in\{1,\cdots,\sqrt{L}/2\}}\ \left(d_m^{Im_i}\right)\ .$$

The $\sqrt{L}/2$ candidates of $\{d_m^{Re_i}\}_{i=1}^{\sqrt{L}/2}$ and $\{d_m^{Im_i}\}_{i=1}^{\sqrt{L}/2}$ may be evaluated by:

$$\begin{aligned} d_m^{Re_i} &= \Lambda(|t_m^{Re_i}|) + \textstyle\sum_{j=(\log_2 L)/2+2}^{\log_2 L} b_j L_a(b_j) - \frac{A_i^2\mu_m^2}{N_0}, \\ d_m^{Im_i} &= \Lambda(|t_m^{Im_i}|) + \textstyle\sum_{j=2}^{(\log_2 L)/2} b_j L_a(b_j) - \frac{A_i^2\mu_m^2}{N_0}. \end{aligned}$$

(3) The $(\log_2 M)$ bits which determine the antenna activation index may be detected as:

$$L_p(b_k) = \text{jac}_{m\in\bar{\mathbf{m}}_{b_k=1}}(d_m) - \text{jac}_{m\in\bar{\mathbf{m}}_{b_k=0}}(d_m),\quad k\in\{\log_2 L+1,\cdots,\log_2 I\}.$$

(4) The first bit and the $\left(\frac{\log_2 L}{2}+1\right)$-th bit which determine the signs may be detected as:

$$\begin{aligned} L_p(b_1) &= \text{jac}_{m\in\bar{\mathbf{m}}}\left(d_m^{Re} + d_m^{Im,b_1=1} + \text{Pr}_m\right) - \text{jac}_{m\in\bar{\mathbf{m}}}\left(d_m^{Re} + d_m^{Im,b_1=0} + \text{Pr}_m\right), \\ L_p\left(b_{(\log_2 L)/2+1}\right) &= \text{jac}_{m\in\bar{\mathbf{m}}}\left(d_m^{Re,b_{(\log_2 L)/2+1}=1} + d_m^{Im} + \text{Pr}_m\right) \\ &\quad - \text{jac}_{m\in\bar{\mathbf{m}}}\left(d_m^{Re,b_{(\log_2 L)/2+1}=0} + d_m^{Im} + \text{Pr}_m\right), \end{aligned}$$

where $d_m^{Im,b_1=1}$ and $d_m^{Im,b_1=0}$ may be obtained by replacing $\{\Lambda(|t_m^{Im_i}|)\}_{i=1}^{\sqrt{L}/2}$ in Step (2) by $\{-t_m^{Im_i}\}_{i=1}^{\sqrt{L}/2}$ and $\{t_m^{Im_i}\}_{i=1}^{\sqrt{L}/2}$, respectively, while $d_m^{Re,b_{(\log_2 L)/2+1}=1}$ and $d_m^{Re,b_{(\log_2 L)/2+1}=0}$ may be obtained by replacing $\{\Lambda(|t_m^{Re_i}|)\}_{i=1}^{\sqrt{L}/2}$ in Step (2) by $\{-t_m^{Re_i}\}_{i=1}^{\sqrt{L}/2}$ and $\{t_m^{Re_i}\}_{i=1}^{\sqrt{L}/2}$, respectively.

(5) The rest $(\log_2 L-2)$ bits which determine the real PAM magnitudes may be detected as:

$$\begin{aligned} L_p(b_k) &= \text{jac}_{m\in\bar{\mathbf{m}}}\left[d_m^{Re} + \text{jac}_{b_k=1}\ (d_m^{Im_i}) + \text{Pr}_m\right] \\ &\quad - \text{jac}_{m\in\bar{\mathbf{m}}}\left[d_m^{Re} + \text{jac}_{b_k=0}\ (d_m^{Im_i}) + \text{Pr}_m\right],\ k\in\{2,\cdots,(\log_2 L)/2\}, \\ L_p(b_k) &= \text{jac}_{m\in\bar{\mathbf{m}}}\left[\text{jac}_{b_k=1}\ (d_m^{Re_i}) + d_m^{Im} + \text{Pr}_m\right] \\ &\quad - \text{jac}_{m\in\bar{\mathbf{m}}}\left[\text{jac}_{b_k=0}\ (d_m^{Re_i}) + d_m^{Im} + \text{Pr}_m\right],\ k\in\{(\log_2 L)/2+2,\cdots,\log_2 L\}. \end{aligned}$$

TABLE IV

ALGORITHM 4: REDUCED-COMPLEXITY APPROX-LOG-MAP ALGORITHM CONCEIVED FOR GENERAL LPSK/QAM AIDED SM DETECTION.

(1) Define the test-variables as:

$$t_m^{\text{Re}_i} = \frac{A_i \text{Re}(\tilde{Z}_n^m)}{N_0} - \frac{L_a(b_2)}{2},\quad t_m^{\text{Im}_i} = \frac{B_i \text{Im}(\tilde{Z}_n^m)}{N_0} - \frac{L_a(b_1)}{2},$$

where $\{(A_i,B_i)\}_{i=1}^{L/4}$ denote the coordinates of the LPSK/QAM constellation points in the first quadrant.

(2) The *a posteriori* probability of a specific antenna index m is given by:

$$d_m = \text{jac}_{i\in\{1,\cdots,L/4\}}\ (d_m^i) + \text{Pr}_m,$$

where the $L/4$ candidates of $\{d_m^i\}_{i=1}^{L/4}$ are evaluated by:

$$d_m^i = \Lambda(|t_m^{Re_i}|) + \Lambda(|t_m^{Im_i}|) + \textstyle\sum_{j=3}^{\log_2 L} b_j L_a(b_j) - \frac{(A_i^2+B_i^2)\mu_m^2}{N_0}.$$

(3) The $(\log_2 M)$ bits which determine the antenna activation index may be detected as:

$$L_p(b_k) = \text{jac}_{m\in\bar{\mathbf{m}}_{b_k=1}}(d_m) - \text{jac}_{m\in\bar{\mathbf{m}}_{b_k=0}}(d_m),\quad k\in\{\log_2 L+1,\cdots,\log_2 I\}.$$

(4) The first two bits which determine the signs may be detected as:

$$\begin{aligned} L_p(b_1) &= \text{jac}_{m\in\bar{\mathbf{m}}}\ (d_m^{i,b_1=1}) - \text{jac}_{m\in\bar{\mathbf{m}}}\ (d_m^{i,b_1=0}), \\ L_p(b_2) &= \text{jac}_{m\in\bar{\mathbf{m}}}\ (d_m^{i,b_2=1}) - \text{jac}_{m\in\bar{\mathbf{m}}}\ (d_m^{i,b_2=0}), \end{aligned}$$

where $d_m^{i,b_1=1}$ and $d_m^{i,b_1=0}$ may be obtained by replacing $\{\Lambda(|t_m^{Im_i}|)\}_{i=1}^{L/4}$ in Step (2) by $\{-t_m^{Im_i}\}_{i=1}^{L/4}$ and $\{t_m^{Im_i}\}_{i=1}^{L/4}$, respectively, while $d_m^{i,b_2=1}$ and $d_m^{i,b_2=0}$ may be obtained by replacing $\{\Lambda(|t_m^{Re_i}|)\}_{i=1}^{L/4}$ in Step (2) by $\{-t_m^{Re_i}\}_{i=1}^{L/4}$ and $\{t_m^{Re_i}\}_{i=1}^{L/4}$, respectively.

(5) The rest $(\log_2 L-2)$ bits which determine the magnitude of the transmitted LPSK/QAM symbol may be detected as:

$$L_p(b_k) = \text{jac}_{m\in\bar{\mathbf{m}}}\left[\text{jac}_{b_k=1}\ (d_m^i)\right] - \text{jac}_{m\in\bar{\mathbf{m}}}\left[\text{jac}_{b_k=0}\ (d_m^i)\right],\ k\in\{3,\cdots,\log_2 L\}.$$

B. STSK Detection

The received signal model of STSK may also be represented by Eq. (2), where the STSK transmission matrix $\mathbf{S}_n$ has $(T \times M)$ elements, while the received signal matrix $\mathbf{Y}_n$ and the AWGN matrix $\mathbf{V}_n$ are of size $(T \times N)$. Therefore, the hard-decision matrix-by-matrix-based STSK detection is also given by Eq. (3), while the soft STSK detection algorithms may invoke the matrix-by-matrix-based *a posteriori* probability of Eq. (17). In order to operate STSK detection on a vector-by-vector basis, Eq. (2) may be formulated as [8]:

$$\overline{\mathbf{Y}}_n = \mathbf{K}_n \overline{\mathbf{H}}_n + \overline{\mathbf{V}}_n, \tag{41}$$

where the notations are given by:

$$\begin{aligned} &\overline{\mathbf{Y}}_n = [rvec(\mathbf{Y}_n)]^T, && \overline{\mathbf{H}}_n = \chi(\mathbf{I_T} \otimes \mathbf{H}_n), \\ &\mathbf{K}_n = [\underbrace{0 \ \cdots \ 0}_{q-1}, s_l, \underbrace{0 \ \cdots \ 0}_{Q-q}], && \overline{\mathbf{V}}_n = [rvec(\mathbf{V}_n)]^T, \\ &\chi = \left[rvec(\widetilde{\mathbf{A}}_1), \ \cdots, \ rvec(\widetilde{\mathbf{A}}_Q)\right]^T, \end{aligned} \tag{42}$$

while $\otimes$ denotes the Kronecker product. As a result, the new decision metric becomes:

$$\left\|\overline{\mathbf{Y}}_n - \mathbf{K}_i \overline{\mathbf{H}}_n\right\|^2 = \left\|\overline{\mathbf{Y}}_n\right\|^2 + |s_l|^2 \left\|\overline{\mathbf{H}}_n^q\right\|^2 - 2\mathrm{Re}(\overline{\mathbf{Y}}_n \overline{\mathbf{H}}_n^H \mathbf{K}_i^H), \tag{43}$$

where $\left\{\overline{\mathbf{H}}_n^q\right\}_{q=1}^{Q}$ denotes the q-th row in $\overline{\mathbf{H}}_n$, and we have $\left(\left\|\overline{\mathbf{H}}_n^q\right\|^2 = \left\|\widetilde{\mathbf{A}}_q \mathbf{H}_n\right\|^2\right)$. We note that detecting the antenna index m for SM is equivalent to detecting the dispersion matrix index q for STSK. Therefore, the decision metrics seen in Eqs. (7) and (18) should be expressed in the following form for STSK detection:

$$\|\mathbf{Z}_n - \mu_q \mathbf{K}_i\|^2 = \|\mathbf{Z}_n\|^2 + |s_l|^2 \mu_q^2 - 2\mathrm{Re}(\mu_q \mathbf{Z}_n \mathbf{K}_i^H), \tag{44}$$

which is equivalent to Eq. (43). In order to arrive at the appropriate decorrelating vector $\mathbf{Z}_n$ and at the normalization variables $\{\mu_q\}_{q=1}^{Q}$, we further consider STSK in three scenarios:

(1) When we have $(M \leq T)$ and LPSK is employed for STSK, the fading channel's output power in Eq. (43) is given by $\left(\left\|\overline{\mathbf{H}}_n^q\right\|^2 = \mathrm{tr}\{\mathbf{H}_n \mathbf{H}_n^H \widetilde{\mathbf{A}}_q^H \widetilde{\mathbf{A}}_q\} = \|\mathbf{H}_n\|^2\right)$, which is a constant. In such a case, the decorrelating vector is given by $\left(\mathbf{Z}_n = \overline{\mathbf{Y}}_n \overline{\mathbf{H}}_n^H\right)$, while the normalization variables are given by a constant of $\{\mu_q = 1\}_{q=1}^{Q}$.

(2) When we have $(M \leq T)$ and LQAM is employed for STSK, the symbol-power $(|s_l|^2)$ is no longer a constant. Therefore, the decorrelating vector may be obtained by $\left(\mathbf{Z}_n = \overline{\mathbf{Y}}_n \widetilde{\overline{\mathbf{H}}}_n^H\right)$, where the fading channel should be normalized by $(\widetilde{\overline{\mathbf{H}}}_n = \overline{\mathbf{H}}_n/\mu)$, while the normalization variables are given by a constant of $\{\mu_q = \mu = \|\mathbf{H}_n\|\}_{q=1}^{Q}$.

(3) When we have $(M > T)$, the fading channel power of $(\left\|\overline{\mathbf{H}}_n^q\right\|^2)$ is no longer a constant. As a result, we may have the decorrelating vector as $\left(\mathbf{Z}_n = \overline{\mathbf{Y}}_n \widetilde{\overline{\mathbf{H}}}_n^H\right)$, where each row in $\widetilde{\overline{\mathbf{H}}}_n$ should be normalized as $\left\{\widetilde{\overline{\mathbf{H}}}_n^q = \overline{\mathbf{H}}_n^q\right\}_{q=1}^{Q}$, while the normalization variables are given by $\{\mu_q = \left\|\overline{\mathbf{H}}_n^q\right\|\}_{q=1}^{Q}$.

We note that among all the Generalized STSK schemes of [18], only STSK detection may proceed from Eq. (43) to Eq. (44), which allows us to invoke our proposed reduced-complexity SM detector.

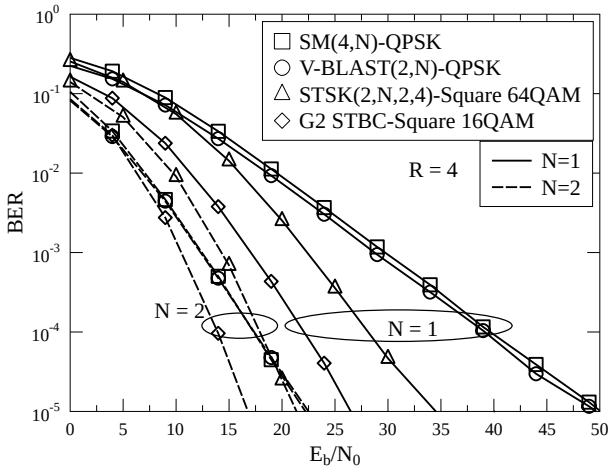

Fig. 2. BER performance of the V-BLAST(2,N)-QPSK, SM(4,N)-QPSK, STSK(2,N,2,4)-Square 64QAM as well as Square 16QAM aided G2 STBC.

V. Performance Results

We provide our simulation results in this section. Our comparison between the reduced-complexity hard STSK detection conceived in Sec. IV and the STSK detection proposed in [1] is portrayed in Fig. 1. The STSK detectors of [1] can only achieve the ML performance when Star LQAM is employed, while the Square LQAM aided STSK detectors impose a performance loss, which is evidenced by Fig. 1(a). By contrast, Fig. 1(a) shows that the new STSK detectors proposed in this work retain their optimal detection capability, despite their substantially reduced complexity. Moreover, in Fig. 1(b) we quantify the complexity imposed in terms of the total number of real-valued calculations required for producing a single-bit decision. Explicitly, the complexity comparison of Fig. 1(b) demonstrates that the proposed STSK detector's complexity is lower than that of its counterparts conceived in [1]. This is a benefit of the fact that the LQAM demodulators were streamlined in the proposed Algorithms 1 and 2. It is also demonstrated in Fig. 1 that although the Star LQAM aided STSK detector using Algorithm 2 has a slightly better BER performance, the Square LQAM aided STSK detection using Algorithm 1 exhibits the lowest detection complexity.

Fig. 2 demonstrates our performance comparison between a range of MIMO schemes associated with the same rate, where the transmission rates of the SM, V-BLAST, STSK and STBC schemes are given by $\log_2(L \cdot M)$, $\log_2(L^M)$, $\log_2(L \cdot Q)/T$ and $\log_2(L^Q)/T$, respectively. When no receive diversity is achieved owing to $(N = 1)$, the SM scheme performs slightly worse than its V-BLAST counterpart, and the STSK scheme has an improved performance as a benefit of its diversity gain, while STBC G2 exhibits the best performance, which is evidenced by Fig. 2. However, Fig. 2 also shows that

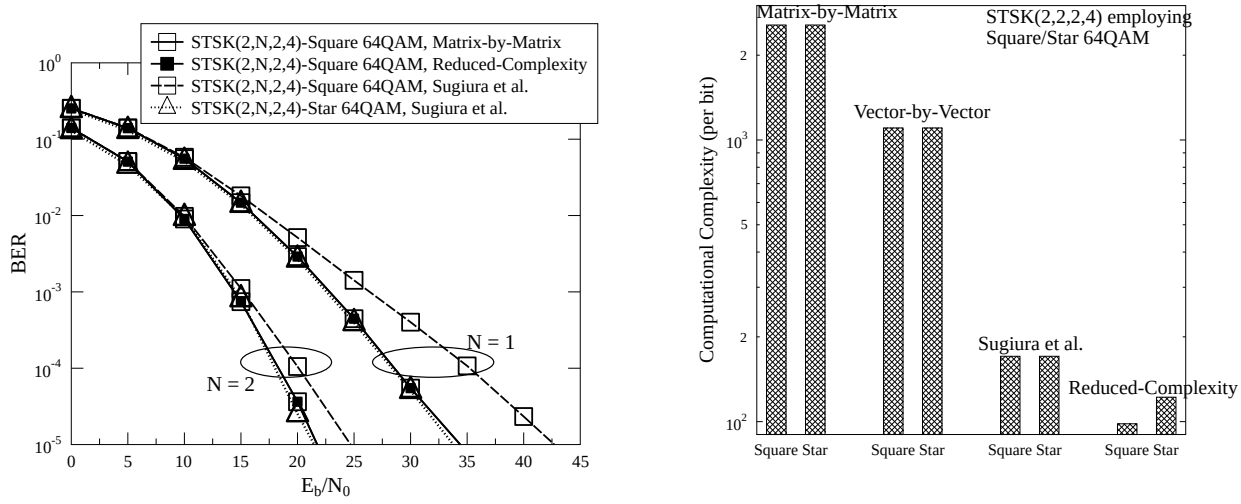

(a) BER performance comparison.

(b) Detection complexity comparison.

Fig. 1. BER performance and detection complexity comparison between the reduced-complexity hard STSK detectors conceived in Sec. IV and the STSK detectors proposed by Sugiura et al. in [1].

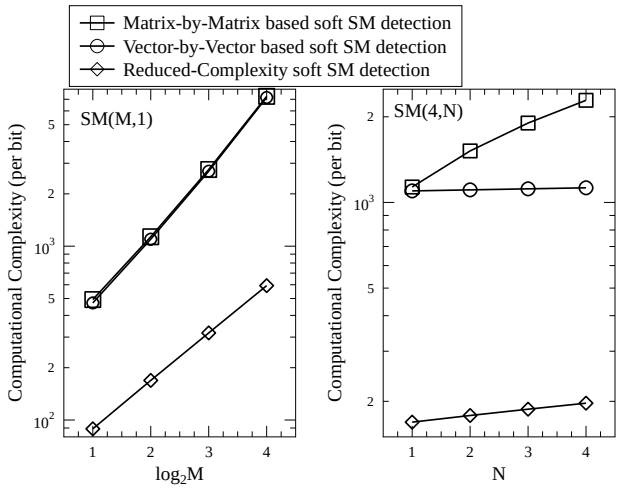

(a) $M = \{2, 4, 8, 16\}$, $N = 1$ (b) $M = 4$, $N = \{1, 2, 3, 4\}$

Fig. 3. Complexity comparison between soft SM detection arrangments when different number of antennas are equipped. Square 16QAM was employed for SM(M,N) scheme, while the Approx-Log-MAP algorithm was invoked for soft SM detection.

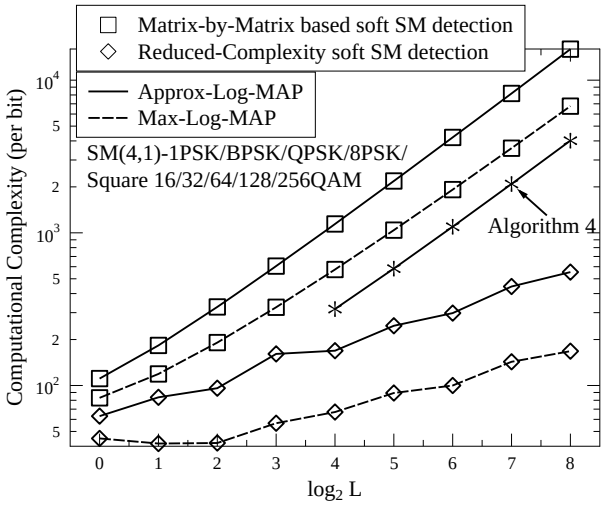

Fig. 4. Complexity comparison between soft SM detection arrangments when different LPSK/QAM scheme was employed for SM(4,1) scheme. The Square LQAM aided SM detection invokes Algorithm 3 with a lower detection complexity, while high-order LPSK, Star LQAM or Cross LQAM aided SM detection invokes Algorithm 4.

as N increases, the SM scheme and the V-BLAST scheme perform better at low SNRs because the STSK scheme and the G2 STBC scheme have to employ high-order QAM in order to compensate for their thoughput loss owing to utilizing T symbol periods for the sake of achieving full diversity.

Our complexity comparisons made for different soft SM detection arrangements are portrayed in Figs. 3 and 4. It can be seen in Fig. 3(b) that following the decorrelating process of Eq. (5), the complexity of both the vector-by-vector based SM detection and of the proposed SM detection no longer grows significantly as N increases. Furthermore, Figs. 3(a) and 4 show that the complexity reduction provided by our proposed soft SM detectors becomes even more substantial as M and L increases. For the SM(4,1)-Square 64QAM scheme, a factor 14 and a factor 19 complexity reduction are achieved by the Approx-Log-MAP and by the Max-Log-MAP, respectively, which is evidenced by Fig 4. Furthermore, as expected, Fig. 4 shows that Square LQAM aided SM detection using Algorithm 3 has a lower detection complexity compared to high-order LPSK, Star LQAM or Cross LQAM aided SM detection using Algorithm 4. Fig. 4 also confirms that Approx-Log-MAP generally has a higher detection complexity than Max-Log-MAP. However, it is widely recognized that Approx-Log-MAP outperforms Max-Log-MAP, and a performance comparison between these two algorithms invoked for STSK

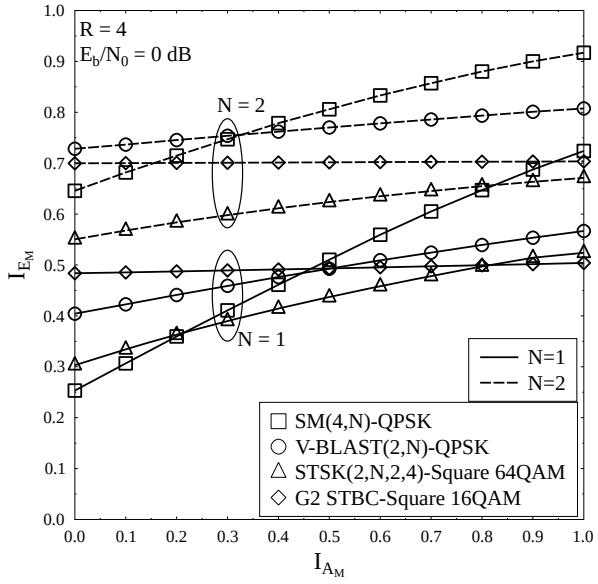

Fig. 5. EXIT charts of the V-BLAST(2,N)-QPSK, SM(4,N)-QPSK, STSK(2,N,2,4)-Square 64QAM as well as Square 16QAM aided G2 STBC.

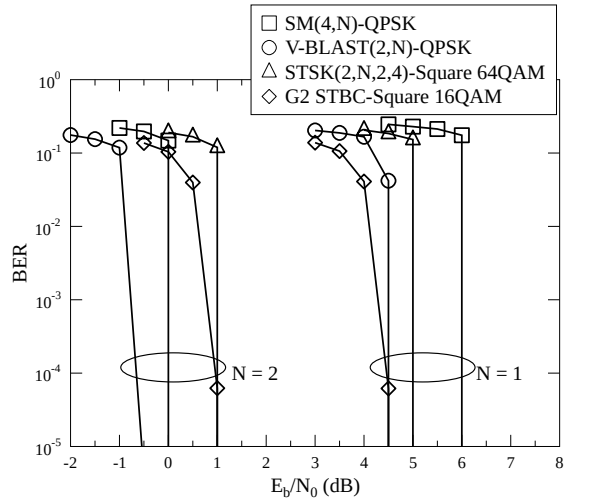

Fig. 6. BER performance of the turbo coded V-BLAST(2,N)-QPSK, SM(4,N)-QPSK, STSK(2,N,2,4)-Square 64QAM as well as Square 16QAM aided G2 STBC.

detection may be found in [2]. We invoke Approx-Log-MAP for all the soft MIMO detectors in the rest of this section.

The EXIT curves of Fig. 5 demonstrate that both the SM and the STSK exhibit an increased iteration gain. Furthermore, Fig. 5 also predicts that the SM scheme and the V-BLAST scheme employing low-level QPSK may perform better with the aid of channel coding, when $(N = 2)$ receive antennas are used. We applied our proposed design in a Turbo Coded (TC) system [19]. Four inner TC iterations ($I_{inner} = 4$) were used, while $(I_{outer} = 5)$ outer iterations were employed for the TC-STSK and TC-V-BLAST systems. Since the SM scheme has a high iteration gain, while the G2 STBC scheme has a near-horizontal EXIT curve in Fig. 5, $(I_{outer} = 10)$ and $(I_{outer} = 2)$ were used by the TC-SM system and the TC-G2 STBC system, respectively. The BER performance of Fig. 6 confirmed our EXIT chart based predictions of Fig. 5.

VI. Conclusions

We have conceived both hard-decision and soft-decision LPSK/QAM aided SM detection. The antenna index and the LPSK/QAM symbol are detected separately, while their correlation is taken into account, so that the optimal performance is retained. Furthermore, our simulation results demonstrate that although the SM/STSK schemes performed slightly worse than the V-BLAST/STBC schemes, they have a substantially reduced detection complexity, which offers them an appealing advantage in realistic MIMO systems.

VII. Appendix

A. Reduced-Complexity Hard-Decision-Aided SSK Detection

The optimum antenna activation index is given by $\hat{m} = \arg \max_{m \in \bar{\mathbf{m}}} \mathrm{Re}(\widetilde{Z}_n^m) - \mu_m^2$.

B. Reduced-Complexity Hard-Decision-Aided BPSK Based SM Detection

The antenna activation index may be found by evaluating $\hat{m} = \arg \max_{m \in \bar{\mathbf{m}}} \left|\mathrm{Re}(\widetilde{Z}_n^m)\right| - \mu_m^2$. Then the BPSK demodulator may be invoked for detecting the sign of $\mathrm{Re}(\widetilde{Z}_n^{\hat{m}})$.

C. Reduced-Complexity Approx-Log-MAP Algorithm Conceived for SSK Detection

The Approx-Log-MAP algorithm conceived for SSK detection is given by Eq. (24), where we have $k \in \{1, \cdots, \log_2 M\}$. The *a posteriori* probability metric of Eq. (24) is given by $d_m = \frac{\mathrm{Re}(\widetilde{Z}_n^m)}{N_0} - \frac{\mu_m^2}{N_0} + \mathrm{Pr}_m$.

D. Reduced-Complexity Approx-Log-MAP Algorithm Conceived for BPSK Aided SM Detection

The $(\log_2 M)$ bits $\{L_p(b_k)\}_{k=2}^{\log_2 M+1}$ which determine the antenna activation index may be detected by Eq. (24). The *a posteriori* probability metric of Eq. (24) is given by $d_m = \Lambda(|t_m^{Re}|) - \frac{\mu_m^2}{N_0} + \mathrm{Pr}_m$, while the test-variable is defined as $t_m^{Re} = \frac{\mathrm{Re}(\widetilde{Z}_n^m)}{N_0} - \frac{L_a(b_1)}{2}$. Furthermore, the first bit, which is assigned to the BPSK symbol may be detected as:

$$L_p(b_1) = \mathrm{jac}_{m \in \bar{\mathbf{m}}} \left(-t_m^{Re} - \frac{\mu_m^2}{N_0} + \mathrm{Pr}_m \right) - \mathrm{jac}_{m \in \bar{\mathbf{m}}} \left(t_m^{Re} - \frac{\mu_m^2}{N_0} + \mathrm{Pr}_m \right). \quad (45)$$

References

[1] S. Sugiura, C. Xu, S. X. Ng, and L. Hanzo, "Reduced-complexity coherent versus non-coherent QAM-aided space-time shift keying," *IEEE Trans. Commun.*, vol. 59, pp. 3090–3101, Nov. 2011.

[2] C. Xu, S. Sugiura, S. X. Ng, and L. Hanzo, "Reduced-complexity soft-decision aided space-time shift keying," *IEEE Signal Process. Lett.*, vol. 18, pp. 547–550, Oct. 2011.

[3] C. J. Foschini, "Layered space-time architecture for wireless communication in a fading environment when using multiple antennas," *Bell Labs. Tech. J.*, vol. 1, no. 2, pp. 41–59, 1996.

[4] S. Alamouti, "A simple transmit diversity technique for wireless communications," *IEEE J. Sel. Areas Commun.*, vol. 16, pp. 1451–1458, Oct. 1998.

[5] L. Hanzo, O. Alamri, M. El-Hajjar, and N. Wu, *Near-Capacity Multi-Functional MIMO Systems(Sphere-Packing, Iterative Detection and Co-operation)*. John Wiley & Sons, May 2009.
[6] L. Hanzo, T. Liew, and B. Yeap, *Turbo Coding, Turbo Equalisation and Space-Time Coding for Transmission over Fading Channels*. Wiley-IEEE Press, 2003.
[7] R. Mesleh, H. Haas, S. Sinanovic, C. W. Ahn, and S. Yun, "Spatial modulation," *IEEE Trans. Veh. Technol.*, vol. 57, pp. 2228–2241, July 2008.
[8] S. Sugiura, S. Chen, and L. Hanzo, "Coherent and differential space-time shift keying: A dispersion matrix approach," *IEEE Trans. Commun.*, vol. 58, pp. 3219–3230, Nov. 2010.
[9] J. Jeganathan, A. Ghrayeb, and L. Szczecinski, "Spatial modulation: Optimal detection and performance analysis," *IEEE Commun. Lett.*, vol. 12, pp. 545–547, Aug. 2008.
[10] J. Jeganathan, A. Ghrayeb, L. Szczecinski, and A. Ceron, "Space shift keying modulation for MIMO channels," *IEEE Trans. Wireless Commun.*, vol. 8, pp. 3692–3703, July 2009.
[11] C. Xu, S. Sugiura, S. X. Ng, and L. Hanzo, "Reduced-complexity non-coherently detected differential space-time shift keying," *IEEE Signal Process. Lett.*, vol. 18, pp. 153 –156, Mar. 2011.
[12] L. Hanzo, S. X. Ng, W. T. Webb, and T. Keller, *Quadrature Amplitude Modulation: From Basics to Adaptive Trellis-Coded, Turbo-Equalised and Space-Time Coded OFDM, CDMA and MC-CDMA Systems, 3rd Edition*. John Wiley & Sons, Sept. 2004.
[13] X. Dong, N. Beaulieu, and P. Wittke, "Error probabilities of two-dimensional M-ary signaling in fading," *IEEE Trans. Commun.*, vol. 47, pp. 352–355, Mar. 1999.
[14] T. May, H. Rohling, and V. Engels, "Performance analysis of Viterbi decoding for 64-DAPSK and 64-QAM modulated OFDM signals," *IEEE Trans. Commun.*, vol. 46, pp. 182–190, Feb. 1998.
[15] P. Vitthaladevuni, M.-S. Alouini, and J. Kieffer, "Exact BER computation for Cross QAM constellations," *IEEE Trans. Wireless Commun.*, vol. 4, pp. 3039–3050, Nov. 2005.
[16] W. Koch and A. Baier, "Optimum and sub-optimum detection of coded data disturbed by time-varying intersymbol interference," in *IEEE Global Telecommun. Conf. (GLOBECOM'90)*, pp. 1679–1684, vol. 3, Dec. 1990.
[17] P. Robertson, E. Villebrun, and P. Hoeher, "A comparison of optimal and sub-optimal MAP decoding algorithms operating in the log domain," in *IEEE International Conf. Commun. (ICC'95)*, vol. 2, pp. 1009–1013 vol. 2, June 1995.
[18] S. Sugiura, S. Chen, and L. Hanzo, "Generalized space-time shift keying designed for flexible diversity-, multiplexing- and complexity-tradeoffs," *IEEE Trans. Wireless Commun.*, vol. 10, pp. 1144–1153, Apr. 2011.
[19] C. Berrou and A. Glavieux, "Near optimum error correcting coding and decoding: Turbo-codes," *IEEE Trans. Commun.*, vol. 44, pp. 1261–1271, Oct. 1996.

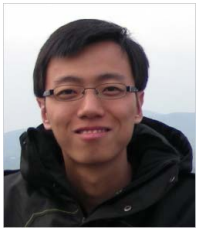

Chao Xu (S'09) received a B.Eng. degree from Beijing University of Posts and Telecommunications, Beijing, China, and a BSc(Eng) with First Class Honours from Queen Mary, University of London, London, UK, through a Sino-UK joint degree program in 2008, both in Telecommunications Enginneering with Management. In 2009, he obtained a MSc degree with distinction in radio frequency communication systems from the University of Southampton, Southampton, UK, and he was awarded IEEE Communications Society UK&RI Chapter Best MSc Student in Broadband and Mobile Communication Networks. He is currently working towards the PhD degree with the Research Group of Communications, Signal Processing and Control, School of Electronics and Computer Science, University of Southampton, UK. His research interests include reduced-complexity MIMO design, non-coherent space-time modulation detection, EXIT-chart-aided turbo detection as well as cooperative communications.

Shinya Sugiura (M'06-SM'12) received the B.S. and M.S. degrees in aeronautics and astronautics from Kyoto University, Kyoto, Japan, in 2002 and 2004, respectively, and the Ph.D. degree in mobile communications from the University of Southampton, Southampton, U.K., in 2010. Since 2004, he has been with Toyota Central R&D Laboratories, Inc., Aichi, Japan, where his research has covered a range of areas in wireless communications, networking, signal processing, and antenna design. He authored/coauthored more than 45 refereed research publications, including 21 IEEE journal and magazine papers.

Dr. Suguira has received a number of distinctions, including the 2011 IEEE Communications Society Asia-Pacific Outstanding Young Researcher Award, the 2011 Ericsson Young Scientist Award, and the 2008 IEEE Antennas and Propagation Society Japan Chapter Young Engineer Award.

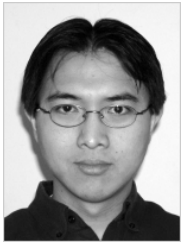

Soon Xin Ng (S'99-M'03-SM'08) received the B.Eng. degree (First class) in electronics engineering and the Ph.D. degree in wireless communications from the University of Southampton, Southampton, U.K., in 1999 and 2002, respectively. From 2003 to 2006, he was a postdoctoral research fellow working on collaborative European research projects known as SCOUT, NEWCOM and PHOENIX. Since August 2006, he has been a member of academic staff in the School of Electronics and Computer Science, University of Southampton. He is involved in the OPTIMIX and CONCERTO European projects as well as the IU-ATC and UC4G projects. He is currently a senior lecturer at the University of Southampton.

His research interests include adaptive coded modulation, coded modulation, channel coding, space-time coding, joint source and channel coding, iterative detection, OFDM, MIMO, cooperative communications, distributed coding and quantum error correction codes. He has published over 140 papers and co-authored two John Wiley/IEEE Press books in this field. He is a senior member of the IEEE, a Chartered Engineer and a fellow of the Higher Education Academy in the UK.

Lajos Hanzo (M'91-SM'92-F'04) FREng, FIEEE, FIET, Fellow of EURASIP, DSc received his degree in electronics in 1976 and his doctorate in 1983. In 2009 he was awarded the honorary doctorate "Doctor Honoris Causa" by the Technical University of Budapest. During his 35-year career in telecommunications he has held various research and academic posts in Hungary, Germany and the UK. Since 1986 he has been with the School of Electronics and Computer Science, University of Southampton, UK, where he holds the chair in telecommunications. He has successfully supervised about 80 PhD students, co-authored 20 John Wiley/IEEE Press books on mobile radio communications totalling in excess of 10,000 pages, published 1250+ research entries at IEEE Xplore, acted both as TPC and General Chair of IEEE conferences, presented keynote lectures and has been awarded a number of distinctions. Currently he is directing an academic research team, working on a range of research projects in the field of wireless multimedia communications sponsored by industry, the Engineering and Physical Sciences Research Council (EPSRC) UK, the European IST Programme and the Mobile Virtual Centre of Excellence (VCE), UK. He is an enthusiastic supporter of industrial and academic liaison and he offers a range of industrial courses. He is also a Governor of the IEEE VTS. Since 2008 he has been the Editor-in-Chief of the IEEE Press and since 2009 a Chaired Professor also at Tsinghua University, Beijing. For further information on research in progress and associated publications please refer to http://www-mobile.ecs.soton.ac.uk